

Observation of Return Current Effects in a Passive Plasma Lens

R. Govil and W. P. Leemans

Center for Beam Physics, Lawrence Berkeley National Laboratory, Berkeley, California 94720

E. Yu. Backhaus and J. S. Wurtele

Physics Department, University of California at Berkeley, Berkeley, California 94720

(Received 24 March 1999)

Observations of relativistic beam focusing by a passive plasma lens have demonstrated a reduction in focusing strength due to plasma return current. A 50 MeV beam was propagated through a 1–3 cm long plasma with density around 10^{14} cm $^{-3}$. Beam size was measured as a function of propagation distance. For a ratio of collisionless plasma skin depth to beam spot size $k_p \sigma_r = 0.33$, no significant reduction in focusing was observed. Reduced focusing was measured for $k_p \sigma_r = 1.1$, where a significant fraction of the inductively driven return current in the plasma flows within the beam. The observations are in good agreement with an envelope equation model and with particle-in-cell simulations.

PACS numbers: 52.40.Mj, 29.27.Eg, 41.75.Ht

The high electric fields that can be attained in plasmas have generated much interest for acceleration [1], focusing [2], and transport of particle beams. Next generation linear colliders require strongly focused beams to achieve the desired high luminosity [3]. Plasma lenses hold the promise of providing focusing strength on the order of 3–10 MG/cm. This is several orders of magnitude larger than can be produced by current day conventional magnets.

The physical mechanism for focusing of particle beams by passive (no external current) plasmas is the expulsion of plasma electrons from the area occupied by the beam and the focusing of the beam in the net plasma and beam fields. The behavior of the lens can be characterized by the ratio of plasma density n_p to beam density n_b . In an overdense plasma lens where $n_p \gg n_b$, the space charge of the electron beam is fully neutralized by the plasma through the displacement of plasma electrons by the beam electrons, resulting in beam self-focusing through its own magnetic field [4]. In the underdense lens, where $n_p \ll n_b$, all plasma electrons are displaced by the beam electrons, and the focusing force is due to the remaining plasma ions [5].

In addition to radial charge displacement, the changing magnetic flux of a bunch induces a longitudinal return current in the plasma which, by Lenz' law, will flow in the opposite direction to the beam current. The scale length for the radius over which the plasma return current flows is on the order of $c/\omega_p \equiv k_p^{-1}$, where c is the speed of light, $\omega_p = \sqrt{e^2 n_0 / m \epsilon_0}$ is the plasma frequency, n_0 is the plasma density, m is the electron rest mass, and ϵ_0 is the dielectric constant. As discussed below, in the overdense regime, the radial force acting on the electron beam is determined by the net current density (the difference between the beam and plasma return current density). Return current effects on the propagation of electron beams in plasmas should therefore become important when the electron beam size, σ_r , is comparable to or greater than the collisionless plasma skin depth, i.e., $k_p \sigma_r \geq 1$, and should lead to a significant reduction in net current. Previous work has

observed focusing in the regime where return current is not significant [4].

The reduction in focusing caused by the plasma return current can be at times highly desirable. For example, very overdense plasma lenses have been proposed to suppress beamstrahlung [6] during the beam-beam interaction in a high energy collider. Intense low energy beam propagation in plasmas is important for the fast ignitor scheme [7] for plasma fusion. Here, ultrahigh current (>MA), low energy electron beams, generated by the interaction of an intense laser pulse with a plasma, have been suggested as a means of depositing large amounts of energy into compressed, ultrahigh density fusion targets. Currents much larger than the Alfvén current, $I_A = mc^3/e = 17.1$ kA, are needed to achieve proper fusion conditions. The propagation of such intense high current beams through high density plasmas [8] is therefore expected to rely on significant current neutralization by the surrounding plasma.

In this Letter we report results [9] of an experimental study of return current cancellation in overdense plasmas through its effect on beam focusing, and a detailed comparison with analytical and particle-in-cell (PIC) code modeling. The experiments were performed at the Beam Test Facility (BTF) [10] at Lawrence Berkeley National Laboratory (LBNL). The experimental setup is shown in Fig. 1.

Electron bunches with energy of 50 MeV (energy spread 0.2%–0.4%) containing typically 1.3 nC of charge within a 10–15 ps (rms) bunch length were produced by the linear accelerator (linac) injector of the LBNL Advanced Light Source. Bend magnets and quadrupoles (BTF line) transported the beam to a 1.2 m long interaction chamber, which was separated from the transport line by a 7 μ m thick kapton window to allow for high pressures in the chamber.

The electron beam profile was monitored inside the chamber using a scanning optical transition radiation (OTR) system [11]. Backward OTR [12], produced when

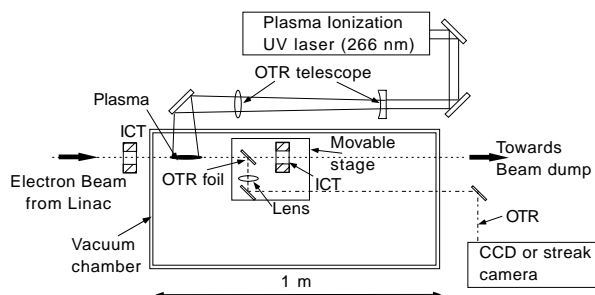


FIG. 1. Experimental setup for the plasma lens experiment. The vacuum chamber is isolated from the beam line with a $7 \mu\text{m}$ thick kapton window and is filled with TPA vapor during plasma lens experiments. ICT's (integrating charge transformer) were used to measure the charge per bunch.

the electron beam hit an aluminum coated fused silica mirror, was collected with a 50 mm diameter, 170 mm focal length lens. The OTR mirror, collection optics, and an ICT were mounted on a 1 m long motorized translation stage. Detailed measurements of the beam size as a function of propagation distance were made by changing the downstream position of the OTR diagnostic setup. After exiting the chamber, the OTR was transported through an 8 m long telescope, providing an image of the electron beam at the radiator location onto a high resolution, 16 bit charge-coupled device (CCD) camera, or on a streak camera with 1.2 ps (rms) temporal resolution. The CCD camera and streak camera were used to measure the time-integrated beam profile as a function of distance and bunch length, respectively. The imaging resolution was $16 \mu\text{m}$.

The unnormalized rms beam emittance ϵ , measured with the OTR scanning system for a fixed quadrupole magnet setting, was 0.3–0.5 mm mrad (rms), where the range was due to day-to-day system variations. Measured bunch duration σ_z (rms) was on the order of 10–15 ps.

Plasmas were produced by laser based two-photon ionization of tripropylamine (TPA) with a frequency quadrupled Nd:YAG laser (266 nm) [13]. The laser beam was focused to a line focus with a spot size on the order of 1 mm high and 1–3 cm wide, using cylindrical lenses at 90° with respect to the electron beam. This geometry allows control over the longitudinal and transverse plasma density profile. After an initial pump down, the vacuum chamber was filled with TPA vapor up to the vapor pressure (3.6 Torr at room temperature). The plasma density was measured using an in-quadrature 94.3 GHz microwave Mach-Zehnder interferometer, capable of providing both phase shift and amplitude variation of the microwave signal through the plasma simultaneously. The microwave beam propagated through the 1 mm thin plasma, orthogonally to the laser beam and electron beam. For laser intensities up to $150 \text{ MW}/\text{cm}^2$ and pressures up to the vapor pressure, the plasma density was found to scale linearly with TPA pressure and quadratically with laser intensity. Densities as high as $5 \times 10^{14} \text{ cm}^{-3}$ were measured. The

measurement of plasma densities higher than the critical density was made possible by detection of the evanescent waves through the finite size plasma (thinner than the microwave skin depth), using the in-quadrature method [13].

Figure 2 shows an example of the change in electron beam shape due to plasma focusing, at a given position inside the experimental chamber (a) without any TPA and (b) with 4.1 Torr laser ionized TPA. The laser produced plasma length was about 1.7 cm with a density of about $2 \times 10^{14} \text{ cm}^{-3}$. The reduction in beam size and increase in intensity are clear indications of plasma lens focusing.

By integrating the total intensity from OTR recorded on the CCD camera and by measuring the beam charge with the ICT's before and after the plasma lens, respectively, we found that no charge was lost.

To study the effect of return current, the ratio of plasma skin depth to beam size was adjusted. This was accomplished by controlling the plasma density through the initial neutral gas pressure as well as the electron beam size at the entrance of the plasma lens, using conventional quadrupole magnets. The peak plasma densities for these two cases were $2.3 \times 10^{13} \text{ cm}^{-3}$ and $2.9 \times 10^{14} \text{ cm}^{-3}$, corresponding to $k_p \sigma_r = 0.33$ and 1.1 and $k_p \sigma_z = 4.1$ and 12.3, respectively. The accuracy of the density measurement was on the order of 25%. The temporal plasma response was therefore adiabatic, which physically means that the current rise was slow compared to the plasma period. For each case, the electron beam size σ_r , time integrated over the electron bunch, was measured as a function of propagation distance z using the scanning OTR system. Horizontal and vertical line profiles through the beam images were found to be well approximated with a Gaussian distribution.

The evolution of the time-integrated transverse electron beam size σ_r versus z was studied through an axisymmetric beam envelope model and a particle-in-cell code. Including only effects of the radial force due to the beam self-fields, plasma response, and the beam emittance, the envelope equation for the azimuthally symmetric beam

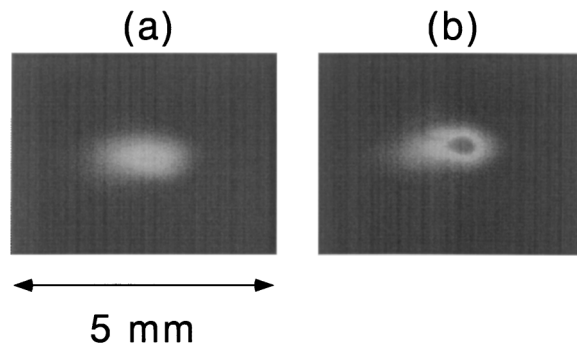


FIG. 2. Time-integrated single shot OTR images at a fixed longitudinal position along the electron beam path in (a) vacuum, and (b) 4.1 Torr of laser ionized TPA. The images were obtained by imaging the OTR with a telescope on a cooled 16 bit CCD camera.

can be written as [14]

$$\frac{\partial^2 \sigma_r}{\partial z^2} - \frac{\varepsilon^2}{\sigma_r^3} - \frac{1}{\gamma m c^2} \frac{\langle r W_r \rangle}{2 \sigma_r} = 0, \quad (1)$$

where $\sigma_r = \sqrt{\langle r^2 \rangle / 2}$, ε is the beam emittance ($\varepsilon = \varepsilon_x = \varepsilon_y$), γ is the relativistic factor, and no acceleration was assumed due to longitudinal wakefields (i.e., $\frac{\partial \gamma}{\partial z} = 0$). The radial wakefield can be written as [15,16]

$$W_r = 4\pi e^2 \left[k_p \int_{-\infty}^{\xi} d\xi' \sin k_p (\xi - \xi') R(r, z, \xi') - \frac{1}{\gamma^2} R(r, z, \xi) \right], \quad (2)$$

with

$$R(r, z, \xi) = -k_p K_1(k_p r) \int_0^r r' dr' n_b(r', z, \xi) I_0(k_p r') + k_p I_1(k_p r) \int_r^{\infty} r' dr' n_b(r', z, \xi) K_0(k_p r'), \quad (3)$$

where $\xi = v_b t - z$ is the distance from the head of the bunch, v_b is the beam velocity in the z direction, and I_0 , I_1 , K_0 , and K_1 are the modified Bessel functions. In the adiabatic limit and when the space charge field of the electron beam is canceled by the plasma, the radial force W_r is due to the magnetic component of the Lorentz force ($\mathbf{v} \times \mathbf{B}$) and can be calculated from the electron beam and induced plasma return current $j_p(r)$,

$$W_r = -e v_b \frac{4\pi}{c^2 r} \int_0^r r' dr' [e v_b n_b(r') - j_p(r')]. \quad (4)$$

To evaluate the average of the radial force, the beam density is assumed Gaussian

$$n_b(r, z, \xi) = \frac{N_b}{(2\pi)^{3/2} \sigma_r^2(z, \xi)} e^{-r^2/2\sigma_r^2(z, \xi) - \xi^2/2\sigma_z^2}, \quad (5)$$

where

$$\langle r W_r(r, z, \xi) \rangle = \frac{1}{\sigma_r^2(z, \xi)} \int_0^{\infty} r dr e^{-r^2/2\sigma_r^2} r W_r(r, z, \xi). \quad (6)$$

In the adiabatic limit, the return current can be calculated from [16]

$$j_p = v_b k_p^2 e \int_0^{\infty} r' dr' n_b(r', z, \xi) I_0(k_p r_{<}) K_0(k_p r_{>}), \quad (7)$$

where $k_p(z) = \omega_p(z)/v_b$ and $r_{<}(r_{>})$ denotes the smaller (larger) of r and r' . The reduction in average focusing force versus $k_p \sigma_r$ is shown in Fig. 3. For the experimental parameters a reduction by about a factor of 2 is expected in changing $k_p \sigma_r$ from 0.33 to 1.1.

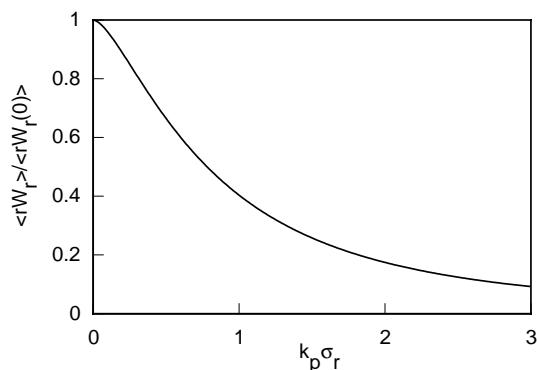


FIG. 3. Ratio of average force including return current effects to the average force in the absence of return currents as a function of $k_p \sigma_r$.

To model the experiment, the initial electron bunch was subdivided into independent longitudinal slices, each with a transverse size $\sigma_r = \sqrt{\langle r^2 \rangle / 2}$ and the envelope equation was solved for each slice. The resulting $\sigma_r(z, \xi)$ were averaged over the beam profile

$$\langle \sigma_r(z) \rangle = \frac{1}{\sqrt{2\pi} \sigma_z} \int_{-\infty}^{\infty} d\xi \sigma_r(z, \xi) e^{-\xi^2/2\sigma_z^2}. \quad (8)$$

To study the effect of the return current, the radial force was evaluated using (a) the full expression [Eqs. (2) and (3)], which includes the contribution to the magnetic field from both the return and beam currents and (b) using the focusing force due solely to the magnetic field of the beam, i.e., ignoring the return current contribution.

In addition to the envelope model, PIC simulations were performed using the fully electromagnetic and relativistic code XOOPIC [17] with two spatial dimensions r, z and three velocity components. The code includes boundary effects. The boundary condition was taken as a cylindrical conducting pipe with the radius much larger than the plasma size. The number of particles in the simulation was $4 \times 10^4 - 8 \times 10^4$ for the beam and $8 \times 10^4 - 4 \times 10^5$ for the plasma. To benchmark the code for beam-plasma systems, electromagnetic fields and electron beam propagation results were compared with known analytical expressions as well as with the envelope equation simulations and found to be in excellent agreement.

For the case where $k_p \sigma_r = 0.33$, Fig. 4(a) shows the measured as well as calculated rms beam envelope radius, including and ignoring the return current effect versus longitudinal position. The experimental measurements are in good agreement with the results from the envelope and the particle-in-cell code XOOPIC, but cannot distinguish between the envelope model with or without the inclusion of the return current. Indeed, for this value of $k_p \sigma_r$, the predicted beam envelope calculated without return current differs only slightly from the results of a calculation with return currents. Only about 12% of the return current flows

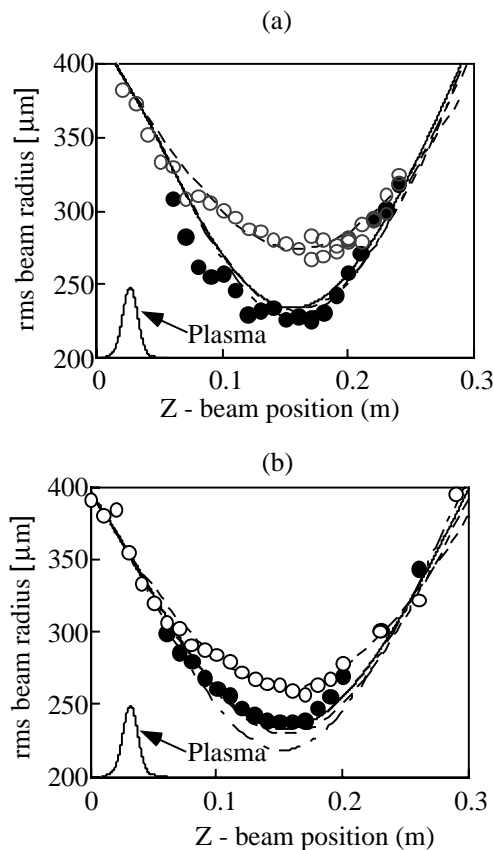


FIG. 4. Measured and predicted values of the rms beam radius are plotted as functions of propagation distance z for (a) $k_p \sigma_r = 0.33$ and (b) $k_p \sigma_r = 1.1$. Two data sets are plotted: measured rms radius after propagating through the TPA gas (hollow dots) and through plasma (solid dots). Each dot represents the average of 10–20 shots and the width of the dot is roughly the error bracket. The solid curves in (a) and (b) correspond to the predictions of the simulation code XOOPIC, the dashed lines the predictions of the full envelope formalism, and the dot-dashed lines the prediction of the envelope formalism without inclusion of return current. Note in (b) the consistently overestimated focusing. The laser ionized plasma with density 2.3×10^{13} for case (a) and $2.9 \times 10^{14} \text{ cm}^{-3}$ for case (b) is centered at $z = 4.4 \text{ cm}$.

within the rms beam area, resulting in a small reduction in focusing strength as seen in Fig. 3.

As seen in Fig. 4(b), for the case where $k_p \sigma_r = 1.1$, the experimental results and the beam envelopes obtained from simulations with XOOPIC are in very good agreement. However, as expected, good agreement between the measurements and the envelope model is obtained only when return currents are included. For this case, approximately 37% of the return current flows inside the rms beam area, causing a significant reduction in magnetic field and hence in the focusing strength (see Fig. 3). The sensitivity to plasma and beam parameters was examined using the model. Changes in plasma density on the order of 25% (i.e., $k_p \sigma_r$ varies by 12%), can be seen from Fig. 3

to have a small effect on the focusing force. Also, it was found to be only weakly sensitive to changes in plasma length, as well as rather insensitive to electron bunch length and charge. The most sensitive parameters were initial spot size and divergence (i.e., emittance) which are fitting parameters.

In summary, return current effects in passive plasma lenses have been observed for the first time. The use of a scanning OTR stage has provided sufficient data statistics enabling detailed comparison between experiment and theory.

We thank L. Archambault, J. Dougherty, W. Byrne, S. Wheeler, and P. Volfbeyn for assistance with the experiment, M. Perry and R. Stevens for loaning the Nd:YAG laser and microwave interferometer, respectively, C.K. Birdsall and J. Verboncoeur for making XOOPIC available, and D. Whittum and E. Esarey for discussions on the envelope equations and return current physics.

-
- [1] For a recent review with many references, see E. Esarey *et al.*, *IEEE Trans. Plasma Sci.* **PS-24**, 252–288 (1996).
 - [2] P. Chen, *Part. Accel.* **20**, 171 (1987).
 - [3] H. Murayama and M.E. Peskin, *Annu. Rev. Nucl. Part. Sci.* **46**, 533 (1996).
 - [4] J.B. Rosenzweig *et al.*, *Phys. Fluids B* **2**, 1376 (1990); H. Nakanishi *et al.*, *Phys. Rev. Lett.* **66**, 1870 (1991); G. Hairapetian *et al.*, *Phys. Rev. Lett.* **72**, 2403 (1995).
 - [5] N. Barov *et al.*, *Phys. Rev. Lett.* **80**, 81 (1998).
 - [6] D.H. Whittum *et al.*, *Part. Accel.* **34**, 89 (1990).
 - [7] M. Tabak *et al.*, *Phys. Plasmas* **1**, 1626 (1994); R.J. Mason and M. Tabak, *Phys. Rev. Lett.* **80**, 524 (1998).
 - [8] A. Pukhov and J. Meyer-ter-Vehn, *Phys. Plasmas* **5**, 1880–1886 (1998).
 - [9] R. Govil, Ph.D. thesis, UC Berkeley, 1998; R. Govil, S. Wheeler, and W.P. Leemans, in *Proceedings of the Particle Accelerator Conference, 1997* (IEEE, Piscataway, NJ, 1997), p. 654.
 - [10] W.P. Leemans *et al.*, in *Proceedings of the Particle Accelerator Conference, 1993* (IEEE, Piscataway, NJ, 1993), pp. 83–85.
 - [11] W.P. Leemans, in *Advanced Accelerator Concepts*, edited by S. Chattopadhyay *et al.*, AIP Conf. Proc. No. 398 (AIP, New York, 1996), p. 23.
 - [12] L. Wartski *et al.*, *J. Appl. Phys.* **46**, 3644–53 (1975).
 - [13] R. Govil, P. Volfbeyn, and W.P. Leemans, in *Proceedings of the IEEE Particle Accelerator Conference, Dallas, Texas, 1995* (IEEE, Piscataway, NJ, 1995), p. 776.
 - [14] E.P. Lee and R.K. Cooper, *Part. Accel.* **7**, 83 (1976).
 - [15] R. Keinigs and M.E. Jones, *Phys. Fluids* **30**, 252 (1987).
 - [16] E.Yu. Backhaus, D. Whittum, and J. Wurtele (to be published).
 - [17] J.P. Verboncoeur, A.B. Langdon, and N.T. Gladd, *Comput. Phys. Commun.* **87**, 199–219 (1995).